Creep, Shrinkage and CTE Evaluation: MoDOT's New

Bridge Deck Mix Companion Testing to HPC Bridge

Deck

By

Dr. John Myers

Nidhi, Joshi

and

Juan La Gamma

University Transportation Center Program at

The University of Missouri-Rolla

**UTC
R85**

Technical Report Documentation Page

1. Report No. UTC R85	2. Government Accession No.	3. Recipient's Catalog No.

4. Title and Subtitle Creep, Shrinkage and CTE Evaluation: MoDOT's New Bridge Deck Mix Companion Testing to HPC Bridge Deck	5. Report Date Feb 2005
	6. Performing Organization Code

7. Author/s Dr. John Myers, Nidhi Joshi and Juan La Gamma	8. Performing Organization Report No. RG001232 OT085

9. Performing Organization Name and Address Center for Infrastructure Engineering Studies/UTC program University of Missouri - Rolla 223 Engineering Research Lab Rolla, MO 65409	10. Work Unit No. (TRAIS)
	11. Contract or Grant No. DTRS98-G-0021

12. Sponsoring Organization Name and Address U.S. Department of Transportation Research and Special Programs Administration 400 7th Street, SW Washington, DC 20590-0001	13. Type of Report and Period Covered Final
	14. Sponsoring Agency Code

15. Supplementary Notes

16. Abstract

MoDOT RDT Research Project R-I00-002 "HPC for Bridge A6130 – Route 412 Pemiscot County" was recently completed in June of 2004 [Myers and Yang, 2004]. Among other research tasks, part of this research study investigated the creep, shrinkage and coefficient of thermal expansion (CTE) of Missouri's first high performance concrete (HPC) superstructure bridge. This study examined these aforementioned properties on both the prestressed concrete (PC) girders and the cast-in-place (CIP) deck which both utilized HPC on this aforementioned project.

In 2003 the Missouri Department of Transportation (MoDOT) studied nine different mix designs for possible use in bridge deck applications [MoDOT Report RI01-044, 2003]. The objective of this internal MoDOT study was to reduce the content of cementitious material to reduce shrinkage, but maintain good durability characteristics. Of the original nine mix designs, one was ultimately selected for use in an actual bridge deck application, namely, MoDOT Bridge A6671 near Waynesville, Missouri. There was interest to study how the mix design used in this bridge compared to the previous HPC deck mix design used in Bridge A6130.

17. Key Words Creep Shrinkage, CTE Bridge Deck, Mix Proportioning, High Performance Concrete	18. Distribution Statement No restrictions. This document is available to the public through the National Technical Information Service, Springfield, Virginia 22161.

19. Security Classification (of this report) unclassified	20. Security Classification (of this page) unclassified	21. No. Of Pages	22. Price

Form DOT F 1700.7 (8-72)

LIST OF CONTENTS

LIST OF FIGURES

LIST OF TABLES

1. INTRODUCTION

1.1 General Description

Creep, shrinkage and coefficient of thermal expansion (CTE) are important for both conventional and high performance concrete (HPC). Creep is defined as continued deformation under a constant stress. Mix composition, curing condition, loading conditions, member geometry, service exposure conditions and amount of reinforcing are major factors affecting creep.

Shrinkage is broadly defined as the decrease in volume of a concrete element as it loses moisture by evaporation. The major factors affecting drying shrinkage are curing conditions, member size, member shape, amount of reinforcing, temperature, and mix composition like aggregate, w/cm ratio, admixtures.

The coefficient of thermal expansion (CTE) of concrete is a function of the coefficients of both the aggregate and paste. Since aggregates generally make up bulk of the concrete mix, the coefficient of thermal expansion of concrete is most influenced by the coefficient of the aggregate, as well as the quantity of aggregate in the mix.

Each of these characteristics is an important consideration when predicting both ultimate strength capacity and serviceability of prestressed concrete elements.

1.2 Project Background and Objective

MoDOT RDT Research Project R-I00-002 "HPC for Bridge A6130 – Route 412 Pemiscot County" was recently completed in June of 2004 [Myers and Yang, 2004]. Among other research tasks, part of this research study investigated the creep, shrinkage and coefficient of thermal expansion (CTE) of Missouri's first high performance concrete (HPC) superstructure bridge. This study examined these aforementioned properties on both the prestressed concrete (PC) girders and the cast-in-place (CIP) deck which both utilized HPC on this aforementioned project.

In 2003 the Missouri Department of Transportation (MoDOT) studied nine different mix designs for possible use in bridge deck applications [MoDOT Report RI01-044, 2003]. The objective of this internal MoDOT study was to reduce the content of

cementitious material to reduce shrinkage, but maintain good durability characteristics. Of the original nine mix designs, one was ultimately selected for use in an actual bridge deck application, namely, MoDOT Bridge A6671 near Waynesville, Missouri. There was interest to study how the mix design used in this bridge compared to the previous HPC deck mix design used in Bridge A6130.

The objectives of this research, project study R-I00-002B, were to:

1. Determine the creep, shrinkage and CTE properties of the MoDOT Bridge A6671 deck mix.

2. Data analysis and curve fitting of the data obtained from MoDOT Bridge A6671 deck mix.

3. Compare the properties with those of the HPC Bridge A6130 (near Hayti, Missouri) deck mix to gain an understanding of the variation that may be expected in these two deck mixes.

The primary difference between the two mix designs was the cementitious content. The coarse aggregate content also varied to some degree.

2. LITERATURE AND BACKGROUND

2.1 Creep

Creep of concrete can broadly be defined as the time-dependent increase in strain under a sustained stress. Total creep actually consists of two components: basic creep and drying creep. Basic creep is the creep occurring with no moisture exchange between the concrete and its surroundings, while drying creep can be defined as the creep dependent on loss of moisture to the environment [Libby, J.R., 1990]. Basic creep is generally associated with the movement and rearrangement of adsorbed water layers, and drying creep is associated with the loss of evaporable water [Ngab, A.S., 1981].

For most engineering applications, it is not necessary to distinguish between basic and drying creep. However, it is important to note that creep and shrinkage are not independent since drying creep is moisture-dependent, and thus influenced by shrinkage [Neville, A.M., 1983]. As a result, creep and shrinkage strains cannot truly be superimposed (i.e. the total time-dependent strain is not equal to the algebraic sum of the basic creep, drying creep, and shrinkage strains). For practical purposes, however, creep can be defined as the time-dependent change in strain of concrete under sustained load, less the shrinkage (and thermal) strain occurring on unstressed concrete in the same environmental conditions. This approach has been used by ACI Committee 209 [1992] and in numerous past experimental studies, and allows for the superposition of creep and shrinkage strains in time-dependent analyses.

It is often useful to quantify creep of concrete in forms other than the total creep strain, ε_c. The two most common forms are specific creep, η_c, and creep coefficient, C_c. Specific creep is sometimes called the "unit creep strain", and is defined as the creep strain per unit stress:

$$\eta_c = \frac{\varepsilon_c}{\sigma} \quad \text{...............................Equation 2.1}$$

The creep coefficient is defined as the ratio of the time-dependent creep strain to the initial elastic strain, ε_i:

$$C_c = \frac{\varepsilon_c}{\varepsilon_i} \quad \text{................................Equation 2.2}$$

Thus, a creep coefficient of 2.0 implies that the total strain due to initial elastic load response and time-dependent creep is three times the initial elastic strain. The specific creep and creep coefficient can be related by the following equation, where E_c is taken as the modulus of elasticity at the time of loading:

$$C_c = E_c \cdot \eta_c \quad \text{..........................Equation 2.3}$$

Many factors have been shown to influence creep of concrete. These factors can generally be categorized as mix composition factors and other factors related to curing, service exposure conditions, loading conditions, and member geometry. Because so many factors influence creep, the magnitude of creep strains will vary greatly between different concretes under different conditions.

Creep essentially occurs in the paste of concrete, and the aggregate acts to restrain the creep of the paste. As a result, the quantity and stiffness (modulus of elasticity) of the coarse aggregate will influence the creep behavior of the concrete to some extent [Neville, A.M., 1981]. Many attempts have been made in the literature to relate creep to water-to-cement (water-to-binder) ratio, cement content, cement type, water content, fine aggregate content, and other paste properties, but the interdependence of such properties has resulted in conflicting data concerning their effects [Mindess, S. and Young, J.F., 1981]. Some authors argue that creep is essentially related to the stress-strength ratio (ratio of the applied stress to the concrete strength at time of loading), which encompasses the net effects of the previously mentioned interdependent paste properties [Neville, 1981 and 1983].

However, it is generally agreed upon that concretes with lower water-to-cement (water-to-binder) ratios exhibit less creep than similar concretes with higher water-to-cement (water-to-binder) ratios. Studies of experimental data have shown this trend to be especially true when corrections are made to account for differences in quantities of cement paste. That is, concretes with lower water-to-cement (water-to-binder) ratios and

the same paste content exhibit lower creep. This conclusion could also be interpreted as demonstrating the influence of water content. Concretes with less water tend to exhibit lower creep.

Loading factors that influence creep behavior include the age of the concrete at loading and magnitude of the applied load. Both of these factors contribute to the stress-strength ratio mentioned in preceding paragraphs. It has been well established that concrete creeps more when loaded at earlier ages. Likewise, higher loads result in more creep strain for a given concrete. A linear relationship between creep strain and magnitude of applied stress is known to exist up to a given level of stress. The upper stress limit of the linear relationship is generally reported as about 50% to 60% of the compressive strength for most concretes. Above this stress, microcracking may occur and the relationship may become nonlinear [Gilbert, R.I., 1988]. At stress levels approaching the ultimate strength of the concrete, creep can eventually lead to failure. The stress level above which this occurs is commonly referred to as the sustained load strength.

Other factors that can influence creep of concrete include curing and service exposure conditions. Duration and type of curing can affect creep by influencing the concrete strength (and thus the stress-strength ratio) at the time of loading. Relative humidity can greatly affect creep, or more precisely, the magnitude of drying creep. Lower relative humidity typically results in significantly increased creep [Neville and Brooks, 1990]. Temperature also influences creep, although for most typical applications it is considered to be a less important environmental factor than relative humidity. Over the range of temperatures applicable to most concrete structures (0 to 70°C [32 to 160°F]), creep increases with increasing temperature [Neville, 1981].

Tests have also shown that the size and shape of a concrete member or specimen can greatly influence its creep, both in terms of the rate of creep and magnitude of ultimate creep [Hansen and Mattock, 1969]. For larger members, the rate of creep and magnitude of ultimate creep are significantly smaller, and the magnitude of total creep approaches the magnitude of basic creep since very little moisture can be lost to the environment. This member size and shape influence has generally been expressed by relating creep to either volume-to-surface ratio, or to a minimum or average member thickness [1992].

There is general agreement that creep is less for high strength concretes than for conventional or normal strength concretes. This trend would be expected given the generally low water-to-cement (water-to-binder) ratios of most high strength concretes. ACI Committee 363 [1992] identifies several studies where less creep was measured for HSC than for comparable normal-strength concretes. Parrot [1969] observed a 25 percent lower creep coefficient in high strength concrete under drying conditions, when compared to normal strength concrete loaded to a similar load ratio (30 percent of the concrete strength). Ngab et al. [1981] found that the specific creep and creep coefficient of high strength concrete with a water-to-cement ratio of 0.32 were respectively 20 to 25 percent and 50 to 75 percent that of normal strength concrete made with similar materials and a water-to-cement ratio of 0.64. Smadi et al. [1987] also observed substantially less creep for high strength concretes with compressive strengths of 59 to 69 MPa (8,500 to 10,000 psi) and a water-to-cement ratio of 0.32, when compared to low and medium strength concretes (compressive strengths less than 41 MPa [6,000 psi]) with water-to-cement ratios of 0.87 and 0.64, respectively.

The Smadi et al. [1987] study also noted that a higher limit exists for high strength concrete for the linear relationship between level of stress and creep strain. This limit was observed to be approximately 65 percent of the compressive strength for HSC, as compared to 45 percent for low and medium strength concretes. Similarly, it was observed that HSC has a higher sustained loading strength. The stress at which creep strains lead to failure was found to be 80 percent of the strength for HSC and 75 percent of the strength for low and medium strength concretes.

The effect on creep of mineral and chemical admixtures, which are commonly used in HPC, is somewhat unclear. Brooks and Neville [1992] suggest that few generalizations can be made concerning their effects on creep, in part because available experimental data covers a wide range of test conditions. It is also important to recognize the indirect effect that admixtures have on creep with respect to the manner in which they influence other creep-influencing parameters (i.e. water-to-cement/water-to-binder ratio, slump/water content, strength, etc.). Nasser and Al-Manaseer [1986] found that creep of 28 MPa (4000 psi) concrete with superplasticizer and 20% Class C fly ash replacement exhibited 72% more creep than the same concrete without admixtures. Sennour and

Carrasquillo [1989] observed a slight increase in creep for concretes with varying percentages of Class C fly ash replacement, and a slight decrease in creep for concretes with Class F fly ash. The difference was attributed to the effect of the varying CaO contents between the two classes of fly ash.

Several models have been proposed for predicting creep as a function of time for a given concrete under a given set of load and exposure conditions. The most common method in use in the United States is probably the ACI 209 [1992] method, which is based on the work of Branson et al. [1971]. This method allows for the determination of an ultimate creep coefficient, C_{cu}, either by experimental tests or by assuming and modifying a base value of 2.35. This base value was determined by analyzing the results of 120 specimens from several experimental studies conducted prior to 1970 on normal-weight, lightweight, and sand-lightweight concretes [Branson, D.E., 1971]. The assumed base value is meant to represent a general average for many concretes, and should be modified using a set of multipliers developed for various factors related to concrete composition. These factors include slump, fine aggregate percentage, cement content, and air content. The multipliers corresponding to these factors may be found in the ACI 209 Committee Report [1992].

The corrected (assumed) or experimentally determined ultimate creep coefficient is then modified using multipliers corresponding to loading, curing, and environmental conditions. The multiplier for ambient relative humidity is given as:

$$\gamma_{rh} = 1.27 - (0.0067 \cdot H) \quad \text{for} \quad H \geq 40 \quad ....\text{Equation 2.4}$$

where H is the relative humidity in percent. The multiplier γ_{rh} defaults to 1.0 for a "standard" relative humidity of 40 percent. For relative humidity less than 40 percent, no equation is given, but γ_{rh} must be taken as greater than 1.0.

A multiplier for size and shape effects may be applied in one of two forms, one related to average member thickness and another related to volume-to-surface ratio. The multiplier corresponding to average member thickness is given as:

$$\gamma_{at} = 1.10 - (0.017 \cdot h) \quad \ldots\ldots\ldots\ldots\ldots\text{Equation 2.5}$$

for ultimate creep values, where h is specified as the average member thickness (in inches) of the part of the member under consideration. The constants 1.10 and 0.017 are replaced by 1.14 and 0.023, respectively, to correct creep values during the first year after loading. This modification is intended to reflect the greater influence of average member thickness during the first year after loading.

The multiplier for size and shape effects based on volume-to-surface ratio, v/s (in inches), is given by:

$$\gamma_{vs} = \tfrac{2}{3} \cdot \left[1 + 1.13 \cdot e^{(-.54 \cdot \frac{v}{s})} \right] \quad \ldots\ldots\ldots\ldots\ldots\text{Equation 2.6}$$

Note that this multiplier becomes 1.0 for the "standard" volume-to-surface ratio of 1.5 (in.).

A correction factor is also suggested to account for loading ages other than 7 days for moist-cured concrete and 1 to 3 days for steam-cured concrete. The Equation for this multiplier may be found in the ACI 209 Committee Report [1992].

Once all appropriate correction factors have been applied, the creep coefficient at any time t, C_{ct}, can be determined as a function of the corrected ultimate creep coefficient, C_{cu}. The following hyperbolic-power expression is used for the relationship, where t is the time in days after casting and t_0 is the time of loading:

$$C_{ct} = \frac{(t - t_0)^{0.6}}{10 + (t - t_0)^{0.6}} \cdot C_{cu} \quad \ldots\ldots\ldots\ldots\text{Equation 2.7}$$

The form of Equation 2.7 is based on the work of Branson et al. [1971]. The coefficients 10 and 0.6 were determined as average values from a set of 120 creep tests. A suggested range of other possible values for these two coefficients, as well as for the ultimate creep coefficient, is provided in the ACI 209 Committee Report [1992]. The general form of Equation 2.7 is given in Equation 2.8:

$$C_{ct} = \frac{(t-t_0)^c}{d+(t-t_0)^c} \cdot C_{cu} \quad ....Equation\ 2.8$$

Other well-known design-oriented prediction models for creep of concrete include the 1990 CEB model [1991] and the simplified BP (Bazant-Panula) model [1980]. The 1990 CEB model is very similar to the ACI 209 model, and allows for the prediction of creep as a function of loading age, loading duration, cement type, relative humidity, and member size and thickness. One of the primary differences between this model and the ACI 209 model is that concrete strength is also considered as a variable in the prediction of creep. A second major difference is that the effects of relative humidity and member size and thickness on the rate of creep are considered, in addition to the effect of these variables on the total or ultimate creep. The lack of consideration of the effects of these variables on the rate of creep is one of the major deficiencies of the ACI 209 model.

The simplified Bazant-Panula [1980] model is a simplified form of a complex model for the prediction of creep. This model was developed using a large database of measured creep values from experimental tests. The interrelation of creep and shrinkage is considered in the BP model, and total creep is separated into terms representing basic creep and drying creep. One of the interesting features of this model is that concrete strength is the major variable in the model, and appears in the calculation of several parameters used in the model.

2.2 Shrinkage

Shrinkage can be broadly defined as the decrease in volume (not related to thermal effects) of hardened concrete with time. In this sense, shrinkage in hardened concrete is to be distinguished from plastic shrinkage, which occurs in concrete prior to setting. Three basic types of shrinkage are generally considered to contribute to the total time-dependent decrease in volume. Drying shrinkage is a result of the loss of moisture over time, carbonation shrinkage is due to the chemical reaction of hardened cement paste with atmospheric carbon dioxide, and autogenous shrinkage is due to a self-desiccating effect that occurs during hydration [Mast, R.F., 1989].

Drying shrinkage is generally considered to be the major component of the total shrinkage in concrete structures [Libby, J.R., 1990]. Still, carbonation shrinkage can greatly increase the total shrinkage under certain environmental conditions, namely the presence of high concentrations of CO_2 at intermediate relative humidities. It is also suggested that many of the experimental data on drying shrinkage include the effects of carbonation shrinkage. Autogenous shrinkage, on the other hand, is typically very small [Neville, 1990]. Fortunately, it is unnecessary to distinguish between these three types of shrinkage in structural design. Thus, the generic term shrinkage will be used throughout the rest of this report.

As with creep, a number of factors are known to affect shrinkage of concrete. These factors can generally be classified as factors related to mix composition, those related to curing and service exposure conditions and those related to size and shape of the member.

Shrinkage is a property of the paste in concrete. Since the aggregate acts to restrain the shrinkage of the paste, it plays a major role in determining the magnitude of concrete shrinkage [Mindess, 1981 and Neville 1985]. The proportion of aggregate in the mix, as well as the stiffness (modulus of elasticity) of the aggregate, are considered by many to be the most important mix composition factors influencing concrete shrinkage. Water-to-cement (water-to-binder) ratio is also generally believed to be proportional to shrinkage, with lower ratios resulting in concrete with lower shrinkage. Water content itself is accepted to be proportional to shrinkage, but there is disagreement as to whether its influence is direct or indirect. Neville suggests that water content only affects shrinkage in that it influences the proportion of aggregate in the mix. Nilson and Winter [1991] suggest that the influence is more direct, and that the quantity of mix water is the chief mix-related factor influencing shrinkage. Their observations are based largely on the linear relationship between mix water and shrinkage strain shown by Troxell et al.[1968].

Curing and environmental exposure factors can greatly influence concrete shrinkage. Elevated curing temperatures have been shown to reduce long-term shrinkage in several studies [Hanson, 1964, Klieger, 1987 and Sennour, 1989]. Some studies [Swamy 1987] have also indicated that the duration of moist curing can influence long-term shrinkage, and ACI Committee 209 [1992] suggests a modification factor that implies less shrinkage for longer moist curing periods. Ambient relative humidity under service conditions is

known to greatly affect concrete shrinkage, primarily because it influences the rate of moisture exchange between the concrete and the surrounding atmosphere. Low relative humidities lead to increased shrinkage. It would similarly be expected that elevated temperatures would accelerate drying and thus increase the rate of shrinkage [Gilbert, 1988], but this effect is considered to be much less significant than the effect of relative humidity [ACI 209, 1992].

One of the most significant factors influencing concrete shrinkage is the size and shape of the member. Both the rate of shrinkage and the ultimate shrinkage tend to decrease as the member becomes larger [Hansen, 1966]. In smaller (thinner) members, the shrinkage tends to occur rapidly and relatively uniformly. In larger (thicker) members, the rate of shrinkage will be fast near the surface, while shrinkage at the innermost parts of the member may develop very slowly or even be nonexistent. Stresses may develop in large members as a result of this differential shrinkage [Mindess, 1981]. The relationship between member geometry and shrinkage is generally modeled using the volume-to-surface ratio, or the average or minimum member thickness.

Experimental data has generally shown no clear trend with respect to shrinkage of high strength concrete, though it is often suggested that the shrinkage of high strength concrete is similar to the shrinkage of normal strength concretes [ACI 363, 1992]. Ngab et. al. [1981] noted slightly higher shrinkage for high strength concrete when compared to normal strength concrete made with similar materials. Smadi et al. [1987] also observed higher shrinkage for high strength concrete (59 to 69 MPa [8,500 to 10,000 psi]) as opposed to normal strength concrete (35 to 41 MPa [5,000 to 6,000 psi]), but observed less shrinkage for HSC than for concretes with very low strengths concrete (21 to 24 MPa [3,000 to 3,500 psi]). Swamy and Anand [1973] observed a high initial rate of shrinkage for high strength concrete made with finely ground Portland cement, but noted that shrinkage strains after two years were approximately equal to values suggested in the CEB code [1970].

There are also few conclusions regarding the shrinkage of high performance concrete (with or without high strengths), or regarding the effect of mineral and chemical admixtures on concrete shrinkage. Brooks and Neville [1992] acknowledge that the effects of individual admixtures are difficult to identify, and that the small body of

experimental data indicates varying results. Sennour and Carrasquillo [1989] noted that the partial replacement of cement with both Class C and Class F fly ashes resulted in a slight increase in shrinkage, and that greater percentages of replacement led to greater increases in shrinkage. El Hindy et. al. [1994] observed less shrinkage in HPC with a water-to-binder ratio of 0.22 and made using a blended cement (7 to 8 percent silica fume by weight) than in HPC with a water-to-binder ratio of 0.28 and no silica fume.

Several models have been proposed for the prediction of concrete shrinkage with time, most of which incorporate the effects of curing and environmental conditions and member geometry (size and shape). Some models also consider the effect of mix composition on shrinkage. The most widely used model in the United States is probably the ACI 209 [1992] method, which was developed by Branson et. al. [1971]. This method recommends an ultimate shrinkage strain of 780 $\mu\varepsilon$ based on an analysis of results from 356 experimental tests conducted on normal, lightweight, and sand-lightweight concretes [Brooks, J.J., 1992]. This base value can be modified by a set of multipliers corresponding to mix composition, or an ultimate shrinkage strain can be determined from experimental tests. Mix composition multipliers may be found in the ACI 209 Committee Report [1992], and include considerations for slump, fine aggregate percentage, cement content, and air content.

The ultimate shrinkage strain is then modified using multipliers that account for relative humidity, member size and shape, and duration of moist curing. These multipliers are similar to those given for creep in Section 2.1, and the notation is consistent. The multiplier for average ambient relative humidity is given in Equation 2.9 and Equation 2.10.

$$\gamma_{rh} = 1.40 - (0.010 \cdot H) \quad \text{for} \quad 40 \le H \le 80 ....Equation\ 2.9$$

$$\gamma_{rh} = 3.00 - (0.030 \cdot H) \quad \text{for} \quad H > 80 ....Equation\ 2.10$$

Note that the multiplier becomes 1.0 for the "standard" relative humidity of 40 percent, and zero for a relative humidity of 100 percent (implying no shrinkage). No Equation is given for relative humidities less than 40 percent, but the multiplier must be taken as greater than 1.0 in this case.

As for creep, the effect of size and shape effects may be considered by using a multiplier for either average member thickness or for volume-to-surface ratio. The multiplier for average member thickness is:

$$\gamma_{at} = 1.17 - (0.029 \cdot h) ....Equation\ 2.11$$

for ultimate shrinkage values. The constants 1.17 and 0.029 are replaced by 1.23 and 0.038, respectively, to correct shrinkage values during the first year of drying. This modification reflects the greater influence of member thickness during the first year of drying.

The multiplier for size and shape effects based on volume-to-surface ratio v/s (in inches) is given by:

$$\gamma_{vs} = 1.2 \cdot e^{\left(-.12 \cdot \frac{v}{s}\right)} ....Equation\ 2.12$$

Note that this multiplier is equal to 1.0 for the "standard" volume-to-surface ratio of 1.5 inches.

A loading factor to account for the duration of moist curing is given in tabular form in the ACI 209 Committee Report [1992]. This factor allows for a reduction in shrinkage with moist curing periods greater than 7 days.

Following the application of all appropriate correction factors, the shrinkage strain $\varepsilon_{sh,t}$ (at any time t after the time t_1 in which drying begins), can be determined as a function of the corrected ultimate shrinkage strain $\varepsilon_{sh,u}$. The same hyperbolic-power expression used for the creep-time relationship is used, with a power of 1.0 and a time coefficient in the denominator of 35:

$$\varepsilon_{sh,t} = \frac{(t-t_1)}{35+(t-t_1)} \cdot \varepsilon_{sh,u} \quad ....\text{Equation 2.13}$$

The coefficient 35 is intended for use with moist-cured concrete, and should be replaced with 55 for steam-cured concrete. The form of Equation 2.14 was suggested by Branson et. al. [1971], and the coefficients were determined as average values from a set of 95 experimental tests. A suggested range of values for the general form of the shrinkage-time equation, given in Equation 2.14, is provided in the ACI 209 Committee Report:

$$\varepsilon_{sh,t} = \frac{(t-t_1)^e}{f+(t-t_1)^e} \cdot \varepsilon_{sh,u} \quad ....\text{Equation 2.14}$$

Other design-oriented prediction models for shrinkage include the 1990 CEB model [1991] and the simplified BP (Bazant-Panula) model [1980]. The CEB model is similar to the ACI 209 approach, and includes considerations for the effects of concrete strength, cement type, relative humidity, and member size. Concrete strength is not meant to be a variable itself, but is included to represent the effects of water-to-cement (water-to-binder) ratio and water content, since most designers will not know these mix composition parameters [Muller, H.S., 1992]. Unlike the ACI 209 approach, the effects of member size on the rate of shrinkage are considered in the CEB model. The simplified Bazant-Panula model is a bit more complex, and considers several mix composition parameters, including sand-to-aggregate ratio, gravel-to-sand ratio, and water-to-cement (water-to-binder) ratio. The BP model also considers the interrelation of creep and shrinkage.

2.3 Coefficient of Thermal Expansion

The coefficient of thermal expansion of concrete is a function of the coefficients of both the aggregate and paste. However, because aggregates generally make up the bulk of the concrete mix, the coefficient of thermal expansion of concrete is most influenced by the coefficient of the aggregate, as well as the quantity of aggregate in the mix. The coefficients of individual aggregates vary greatly with mineralogical composition, but range from about 4 to 13 $\mu\varepsilon/°C$ (2.2 to 7.2 $\mu\varepsilon/°F$). Values for various aggregates are

given by Mindess and Young [1981]. The coefficient of thermal expansion for cement paste is substantially higher than for aggregates, such that the resulting coefficients of expansion for concrete will be higher than for the aggregate alone.

Mindess and Young report a range of coefficients of thermal expansion for concrete of 7.4 to 13 $\mu\varepsilon/°C$ (4.1 to 7.3 $\mu\varepsilon/°F$). ACI Committee 209 [1992] suggests a range of 8.5 to 11.7 $\mu\varepsilon/°C$ (4.7 to 6.5 $\mu\varepsilon/°F$) be used for ordinary thermal stress calculations in the absence of known data, with an average value of 10.0 $\mu\varepsilon/°C$ (5.5 $\mu\varepsilon/°F$). An average coefficient of 11 $\mu\varepsilon/°C$ (6 $\mu\varepsilon/°F$) is specified by AASHTO for use in all calculations [1994, 1998 and 1996].

There is little data available on the coefficient of thermal expansion for high strength or high performance concretes. It is suggested, however, that the thermal properties of high strength concretes are similar to those of conventional concretes [ACI 209, 1992].

Moisture content is also known to have a significant effect on the coefficient of thermal expansion for concrete [Mindess, 1981 and Neville, 1981]. The coefficient is minimum in the unsaturated or fully saturated conditions, and is maximum at intermediate moisture conditions. The influence of moisture content is a result of the internal rearrangement of water molecules between capillary and gel pores as temperature increases. This rearrangement of water adds an additional component of expansion under increasing temperatures, leading to a higher coefficient of thermal expansion. Since the rearrangement of water molecules is not possible in the unsaturated and fully saturated conditions, the coefficient of thermal expansion is minimized in these cases.

3. MATERIAL FABRICATION AND DESIGN

3.1 Specimen Fabrication and Design

Twelve long specimens were cast from sampled concrete on the date of the deck casting, in four groups of samples, each sample approximately one hour after each other. For denomination of the specimens the following was used: The first number designates the group ID, and the second number identifies the particular specimen from that sample group. The specimens with identication numbers are listed in Table 3.1. All of them were air cured. In the beginning we used the twelve specimens for shrinkage readings, as this started before the CTE and creep test. One creep specimen, specimen 1-1 cracked during shipment, but it could still be used for shrinkage measurement. Also one CTE test specimen cracked, but since one additional specimen was fabricated for each required test in the event of shipment damage, this didn't impact the research in any fashion. The Table 3.1 lists each individual test and specimen identification number.

Table 3.1 Specimens for C/S/T

Test	Specimens
Creep	2-1, 3-1, 4-1
Shrinkage	1-1, 1-2, 1-3, 2-1, 2-2, 2-3, 3-1, 3-2, 3-3, 4-1, 4-2, 4-3
CTE	1-3, 2-3, 4-3

Creep tests were performed on eleven specimens. ASTM C512 test procedure was followed with a few basic modifications, including the use of 100 x 600 mm (4 x 24 in) cylinder specimens. This specimen diameter was consistent with that used for testing of compressive strength and modulus of elasticity, and assured that the applied loads required for testing were within the range of loads possible using equipment available to the researchers. The length of these specimens allowed for the measurement of surface strains during the test using a DEMEC mechanical strain gauge with a 200 mm (8 in.) gauge length. In addition, the use of a single long specimen instead of stacking multiple short specimens, such as three 100 x 200 mm (4 x 8 in.) cylinders, eliminated difficulties with alignment between specimens during loading.

In general, a total of eight or nine test specimens were cast for each mix. Two of these specimens were loaded for measurement of creep strains. Three specimens were kept unloaded to monitor strains due to drying shrinkage and changes in the testing environment, and two specimens were used for determination of the coefficient of thermal expansion. One or two additional specimens were cast in case any of the specimens were damaged or poorly fabricated.

Specimens for each mix were cast alongside the member at the precast plant or alongside the structure at the jobsite. Precut segments of PVC pipe and specially fabricated aluminum end inserts were used to form the specimens. Concrete was placed in 100 to 150 mm (4 to 6 in.) layers and each layer was rodded 25 times. A set of creep/shrinkage/thermal (C/S/T) specimens, as well as a group of standard cylinders for testing of compressive strength and modulus of elasticity, is shown shortly after casting at the jobsite in Figure 3.1. For the deck, the long cylinders cast for creep (C), shrinkage (S) and coefficient of thermal expansion (T) were damaged during transportation to UMR due to a vehicular accident. Therefore, for deck concrete, three 100×200 mm (4×8 in.) cylinders were stacked as one creep specimen. The broken long specimen could still be used for shrinkage measurement. The length of these specimens allowed for the measurement of surface strains during the test using a DEMEC mechanical strain gauge with a 200 mm (8 in.) gauge length.

Specimens were capped to prevent moisture loss and were stored alongside the structure for 8 to 18 hours and were shipped to the laboratory in UMR. Approximately 24 hours after casting of the specimens, the PVC molds were removed and DEMEC mechanical strain gauge points were fixed to the surface of the specimen using a quick-set epoxy gel. Points were placed as shown in Figure 3.1, such that three surface strain measurements were taken on three "sides", 120° apart, for a total of nine strain measurements per specimen. The specimens were then sulfur capped to ensure smooth ends, and the DEMEC points allowed setting overnight.
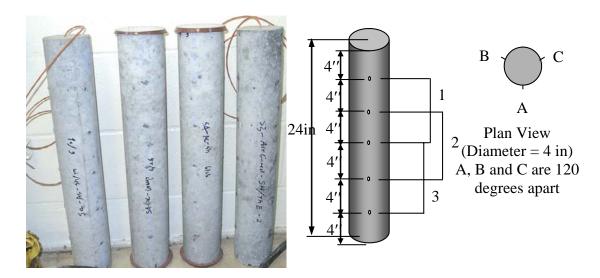
Figure 3.1 C/S/T Specimens and DEMEC Points Arrangement

The loading frames for the creep test are shown in Figure 3.2. They were constructed in accordance with the creep test specification of ASTM. The principle of the design is to apply a constant load to a stack of cylinders between two steel plates by applying pressure with a pump beneath the lower plate and then locking in the load.

Four sets of coil springs were used to each creep rig to maintain the load nearly constant as the specimens shortened. The springs had a maximum compression of 50 mm (2 in.) with an approximate stiffness of 1.612 kN/mm (9.205 k/in). The spring has an inside diameter of 108 mm (4.25 in.) and an outside diameter of 178 mm (7.0 in.). Thus, the total stiffness of the four set of springs was 6.448 kN/mm (36.82 k/in). The rig was designed to support another set of spring so that capacity of the frame can support higher strength concrete at a future time.
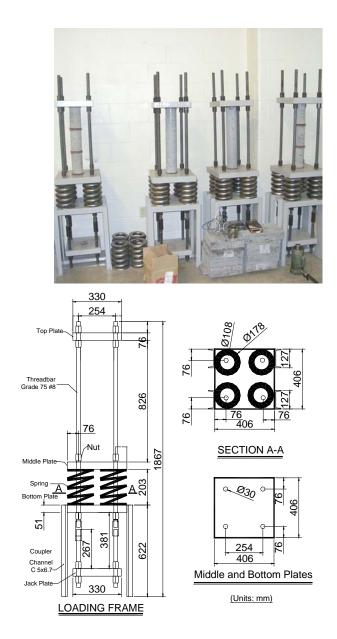
Figure 3.2 Creep Loading Frame and Specimens

A jack and a load cell were used to stress the creep rigs (as shown in Figure 3.3). When the correct load was reached, the nuts below the bottom plate were tightened. The specimens for the HPC girder mix were loaded 2 days after casting to 40% of nominal design compressive strength of the mix. For the cast-in-place specimens, one was air cured in the testing room and the other was moist cured prior to be loaded at 28 days.

Figure 3.3 Creep Loading Frame and Specimens

The applied load for each specimen was maintained throughout the tests using test frames. The loss of load with time, due to the shortening of the specimens and consequential elongation of the springs could be determined by monitoring the spring elongation since the stiffness of the springs was know. When 2% of the initial load was lost, the load was reapplied using the pump and ram.

Readings were taken every day for the first week after loading, every few days for the first 28 days and every few weeks thereafter.

Strains were monitored on the two loaded specimens and three unloaded specimens for each mix. The creep strain for each loaded specimen was determined by subtracting the average strain on the unloaded specimens from the measured strain on the loaded specimen. Measurements were taken every few days for approximately the first 28 days, and every few weeks thereafter for a total duration of at least 180 days.

Shrinkage tests were performed on the sampled mix. Tests were performed in parallel with the creep tests for the mix, and essentially involved the measurement of time-dependent strain on unloaded specimens. Three specimens were typically used for each mix.

As discussed, specimens were transported from the precast plant or jobsite at early ages. Cylinder molds were removed approximately 24 hours after the specimens were cast, and the first strain measurements were typically taken about 24 hours later. The 24

hours between stripping of the molds and the recording of the first strain measurement was necessary to allow adequate time for DEMEC points to be attached and bond to the cylinders. Specimens were air cured during this period.

Strain measurements were recorded on each specimen using a DEMEC mechanical strain gauge with a gauge length of 200 mm (8 in.). The arrangement of DEMEC gauge points on each specimen is shown in Figure 3.1. Measurements were performed simultaneously with measurements on creep (loaded) specimens, usually every few days for the first 28 days and every few weeks thereafter. Readings were taken for a period of at least 180 days.

Because the testing room was not a controlled environment, relative humidity was monitored and found to average 55%. The room temperature also fluctuated, so cylinder temperatures were recorded on selected specimens (at least one from each mix) at the time of each measurement. These temperatures were measured using thermocouples embedded in the specimens during casting.

For each specimen at each measurement interval, the average of the nine individual gauge readings was computed to determine the total strain on the specimen. This total strain represents the strain on the unloaded specimen due to both shrinkage and thermal effects. Temperature strains were then removed analytically using the measured cylinder temperatures and known coefficients of thermal expansion for each mix. In theory, the resulting strain represents the strain due to shrinkage alone.

A correction was also made to all shrinkage measurements to account for the fact that strains could not be measured beginning immediately after the removal of cylinder molds. The first measurements typically were recorded about 24 hours after drying commenced, as this period was required for the placement and bonding of DEMEC mechanical strain gauge points. The analytical correction was made by fitting a regression curve to the measured data, and projecting the curve back for the time period in which drying was occurring but measurements were not being recorded. This analytical correction procedure may be referenced [Myers and Yang, (2004)].

Coefficient of thermal expansion was measured on two specimens for each of the eleven mixes. As for the creep and shrinkage tests, specimens were 100 x 600 mm (4 x

24 in.) cylinders that were cast at the precast plant or jobsite using concrete from the actual bridge structures. Cylinder molds were stripped approximately 24 hours after casting, and specimens were air cured in the room used for creep and shrinkage tests (average RH=55%). Specimens were cured for a minimum of 56 days before testing. This minimized the potential for shrinkage to occur during the actual thermal tests.

Prior to testing, DEMEC mechanical strain gauge points were epoxied to the surface of each specimen as shown in Figure 3.1. Specimens were then pre-cycled to ensure that the specimens had reached the extreme test temperatures at least once prior to actual testing. During testing, specimens were cycled between extreme temperatures of 4.4 °C (40 °F) and 48.9 °C (120 °F). For each set of specimens, two cycles were performed with decreasing temperatures and two cycles with increasing temperatures. Thermocouples placed in the center of the specimens during casting were used to determine when the specimens had stabilized at the extreme temperatures. A standard environmental chamber at UMR was used to control temperature and relative humidity during each test cycle. The relative humidity in the environmental chamber was maintained at 60% throughout the testing.

A set of DEMEC mechanical strain gauge readings was recorded during cycle after specimens stabilized at the extreme temperatures. The internal specimen temperatures were also recorded at the time of each strain measurement. The coefficient of thermal expansion was then determined for each specimen cycle by dividing the change in strain by the change in temperature over the cycle.

3.2 Mix Design Constituents and Proportions

This section focuses on the mix composition and the proportions of different components in the bridge deck mix A6671 and A6130. For bridge deck mix A6671, nine different mixes were initially studied by MoDOT (MoDOT Report RI01-044, 2003) and then one was finalized. The finalized one is listed in Table 3.2. For bridge deck mix A6130, two trial mix and two deck mix batches were studied. The deck mix batch is listed in the Table 3.2. The mix composition and proportions for bridge deck mix A6671 is directly obtained from MoDOT report (MoDOT Report RI01-044, 2003) and the mix

constituents and proportions for bridge deck mix A 6130 is taken from Myers and Yang report [2004].

Table 3.2 illustrates the mix constituents and proportions of the two mixes used in the bridge decks of Bridge A6130 and A6671 respectively. The following draws a comparison between the proportions of different constituents in both bridge deck mixes:

1. The coarse aggregate content of bridge deck mix A6671 was 9.9% higher than bridge deck mix A6130. Based on studies, it has been observed that creep generally occurs in the paste of concrete and aggregate tends to restrain it [Neville & Dilger, 1983]. Therefore, with all other attributes equal less creep and shrinkage can be expected from deck mix A6671.

2. The w/cm ratio is lower for bridge deck mix A6671. It is also generally agreed upon that lower w/cm ratio exhibits lower creep and shrinkage. Therefore, a lower value of creep and shrinkage can be expected from deck mix A6671 compared to that of deck mix A6130 with all other attributes equal. The quantity of water in bridge deck mix A6671 is 10.8% less than that in bridge deck mix A6130.

3. The fly ash used for both bridge deck mixes was an ASTM class 'C' fly ash. The quantity of fly ash in bridge deck mix A6130 was 6.7% higher than that in bridge deck mix A6671. It is expected that this variation in fly ash would not significantly affect the creep and shrinkage.

4. The cement used in both deck mixes was an ASTM Type I Portland cement. The quantity of cement in bridge deck mix A6130 was 30.1% higher than that in A6671. Since creep and shrinkage is influenced by the paste matrix of concrete (cement and water), a higher value of creep and shrinkage can be expected for bridge deck mix A6130 due to higher cement content levels and water levels.

5. GGBFS (blast furnace slag) was used in bridge deck mix A6671 only.

6. A chemical retarder and HRWR (High Range Water Reducer) was used in the deck mix of A6130 only.

7. The quantity of fine aggregate and air entrainment was effectively the same for both the bridge deck mixes.

Table 3.2 Mix Constituents and Proportions for Bridge A6130 and A6671

Mix Proportions		Deck mix A 6130 [Myers and Yang, 2004]	Deck mix A 6671 [MoDOT Report RI01-044, 2003]
Coarse Aggregate	Type	Grad D porphyry for PCCP & Masonry	Potosi Dolomite from Sullivan
	Quantity lbs/cy	1684	1868
Fine Aggregate	Type	Class A Natural Sand	Little Piney River
	Quantity lbs/cy	1078	1080
Water	Type	Potable	Potable
	Quantity lbs/cy	290	258.7
Cement	Type	Type I	Buzzi Unicem (Type I)
	Quantity lbs/cy	558	390
Fly Ash	Type	Class C	Labadie, Mineral resource Tech.
	Quantity lbs/cy	105	98
Microsilica	Type	Microsilica	--
	Quantity lbs/cy	42	N.A.
Retarder	Type	300 R	--
	Quantity lbs/cy	20	N.A.
Air Entrainment	Type	Not reported	Not reported
	Quantity lbs/cy	6	6
HRWR	Type	Not reported	--
	Quantity oz/cy	25	N.A.
GGFBS	Type	--	Buzzi Unicem
	Quantity lbs/cy	N.A.	163
w/cm ratio		0.41	0.39

N.A. – Not Applicable

w/cm – water to cementitious ratio

4. EXPERIMENTAL RESULTS

4.1 Results for Creep Test (Bridge Deck A6671)

This section focuses on the individual and combined behavior of the tested specimens for creep for bridge deck mix A6671. For the concrete deck, strain was measured before and after loading to determine the elastic strain during loading. The raw data obtained from creep tests (for bridge deck mix A6671) was plotted to understand the behavior of each individual specimen and then averaged for three specimens (see Section 3.1). The raw data obtained from creep tests (for bridge deck mix A6671) was then curve fitted for comparison purpose with that of the bridge deck mix of A6130. The primary purpose of this comparison study was to understand the creep and shrinkage behavior of the two bridge deck mixes.

Figure 4.1 below shows the individual behavior of the three specimens (as discussed in experimental test section, chapter 3) instrumented and evaluated for creep. The raw data (of bridge deck mix A6671) obtained from the experiments creep frames is used for plotting and no curve fit is applied to this figure. It is evident from Figure 4.1 that there is irregularity in the graphs over time. This is due to temperature fluctuation in the structural engineering laboratory where the specimens were monitored during the monitoring period.
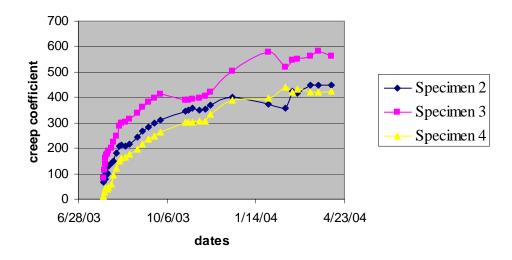

Figure 4.1 Individual Behaviors of Three Creep Specimens (Raw Data)

Figure 4.2 illustrates the combined behavior of the three specimens evaluated for creep (of bridge deck mix A6671) with raw data and the curve fit. For plotting Figure 4.2 the average value of the raw data for the three specimens was taken and the curve fitting was done using Equation 4.1.
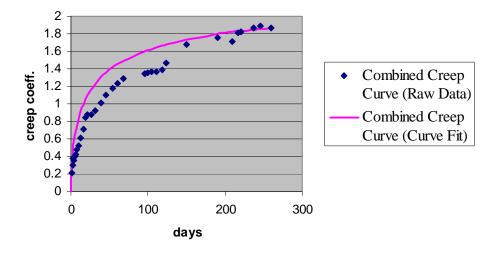

Figure 4.2 Combined Behaviors of Three Creep Specimens (Raw and Curve fit Data)

There are three forms of Equations investigated for curve fitting, namely a general fit, power fixed and parameter fixed. Details on each of these curve fitting methodologies can be referenced in the previous study by Myers and Yang [2004]. Among these the general form was selected because of its improved curve fitting characteristics. Equation 4.1 is the general form equation used for curve fitting and Table 4.1 shows the resulting best fit curve data parameters used in the equation. The value of R^2 obtained from the fitted curve was 0.956.

$$C_{ct} = \frac{(t-t_0)^c}{d + (t-t_0)^c} C_{cu} \quad ....\text{Equation 4.1}$$

where, C_{ct} is the creep coefficient at time t, C_{cu} is the ultimate creep coefficient, c and d are constants.

Table 4.1 Creep-Time Regression Curve Parameters (General Form)

General Form of Equation 4.1				
Bridge deck mix	c	d	C_{cu}	R^2
A 6671	0.6	10	2.4	0.9558

4.2 Results for Shrinkage Test (Bridge Deck A6671)

In this section the results for individual and combined behavior of four shrinkage specimens of bridge deck mix A6671 are plotted (see Section 3.1). The readings were taken for the four specimens at regular intervals. The raw data obtained from shrinkage test (for bridge deck mix A6671) was plotted to understand the behavior of the specimens individually and also in combination. For the comparison and better understanding purpose the raw data is curve fitted.

Figure 4.3 shows the individual behavior for the four individual specimens of bridge deck mix A6671 (see Chapter 2) evaluated for shrinkage; the raw data was used in plotting the figure and no curve fit is applied.
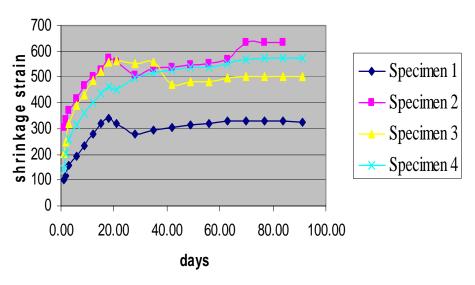

Figure 4.3 Individual Behaviors of 4 Shrinkage Specimens for Deck A6671(Raw Data)

Figure 4.4 shows the combined behavior of shrinkage specimens (of bridge deck mix A6671) with the raw data and the curve fit. Curve fit was done using Equation 4.2 and the parameters are listed in Table 4.2

As mentioned in the Section 4.1, among the three types of regression analysis, general form was used as it fits the data best. Equation 4.2 was used to curve fit the raw data. Table 4.2 shows the parameters used for general fit and the value of R^2 was obtained from the fitted curve.

$$\varepsilon_{sh,t} = \frac{(t\text{-}t_1)^e}{f + (t\text{-}t_1)^e} \varepsilon_{shu} \quad \text{.................Equation 4.2}$$

where, $\varepsilon_{sh,t}$ is the shrinkage at time t, $\varepsilon_{sh,u}$ is the ultimate shrinkage of concrete, e and f are constants.

Table 4.2 Shrinkage-Time Regression Curve Parameters (General Form)

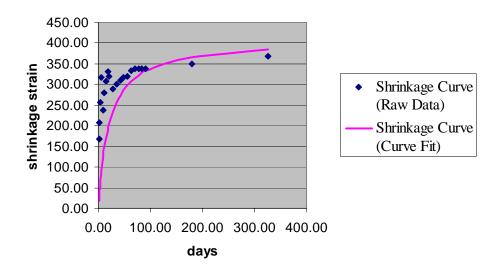| General Form of Equation 4.2				
Average for HPC Girders	e	f	$\varepsilon_{sh,u}$	R^2
	1	21	410	0.9765

Figure 4.4 Combined Behaviors of Four Shrinkage Specimens (Raw Data and Curve Fit)

4.3 Test Results for CTE Test

The Coefficient of Thermal Expansion (CTE) of concrete is a function of the coefficients of both the aggregate and the paste. However, aggregates generally make up the bulk of the concrete mix constituents and therefore the coefficient of thermal expansion of concrete is most influenced by the coefficient of the aggregate, as well as the quantity of aggregate in the mix.

There were 3 specimens (bridge deck mix A 6671) evaluated for coefficient of thermal expansion (see Section 3.1) and the average value of coefficient of thermal expansion was calculated as follows:: $\alpha_t = 5.27 \times 10^{-6}$ 1/F (9.48×10^{-6} 1/C). Further discussion about the CTE is presented in Chapter 5.

5. COMPARISION OF BRIDGE DECK MIX A6671 TO A6130

5.1 Comparison for Creep Results

This chapter discusses the comparison of the results for creep, shrinkage and coefficient of thermal expansion for the sample specimens taken from the bridge deck mixes for Bridges A6671 and A6130.

Table 5.1 shows the creep comparison of the various parameters used in curve fitting and the corresponding R^2 values obtained from the best fit curve for the two bridge deck mixes A6671 and A6130 investigated (see Table 4.1 and 4.2). The values for bridge deck mix A6130 were previously reported by Myers and Yang (2004) and the values for bridge deck mix A6671 were obtained by curve fitting the raw data obtained from experiments (see Section 4.1 and 4.2) conducted in this study. Parameters, for curve fitting of both bridge deck mixes were obtained using Equation 4.1 and 4.2 (general form). The value of R^2 for bridge deck mix A6671 is lower than that of the bridge deck mix A6130. The difference in correlation values may be primarily attributed to the greater degree of temperature variation during monitoring in the laboratory and the wide range of raw data obtained in the experiment of bridge deck mix A6671. However, it should be noted that both R^2 values are quite high indicative of a high level of curve fit.

Table 5.1 Comparison of Creep-Time Regression Curve Parameters (General Form)

Bridge deck mix	c	d	C_{cu}	R^2
A6671	0.6	10	2.4	0.954
A6130	0.4	8.4	4.53	0.993

Figure 5.1 shows comparison of creep coefficients obtained for the HPC deck mix from Bridge A6671 to that of Bridge A6130. The relationship which is shown for both bridge deck mixes represents a comparison of the curve fit equations obtained based on experimental data.
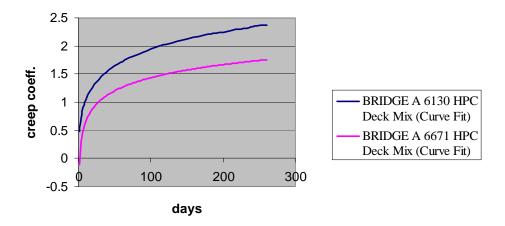
Figure 5.1 Creep Comparison Curve

From the curve fit equations shown in Figure 5.1, the creep coefficient value for bridge deck mix A6671 is 1.78 and for bridge deck mix A6130 is 2.21. The creep coefficient for bridge deck mix A6671 was 19.3% lower than that of the bridge deck mix A6130. As discussed earlier (see Section 1.1) the factors affecting the creep coefficient are largely dependent on mix composition, curing conditions, loading conditions, water cement ratio and others. As observed from the mix constituents and proportions (see Section 3.2), the coarse aggregate was 9.9% higher in bridge deck mix A6671 compared to that of bridge deck mix A6130. Since creep occurs in the paste of concrete and the aggregate tends to restrain it, a lower creep value for bridge deck mix A6671 was somewhat expected and was the case. Moreover, creep is largely influenced by the cement content and w/cm ratio, therefore in general the higher the cement content and w/cm ratio, the higher the creep coefficient. The cement content and the w/cm ratio were higher in bridge deck mix A6130 than that for bridge A6671, resulting in higher value of creep coefficient.

5.2 Comparison of Shrinkage Results

Table 5.2 shows the comparison of the shrinkage parameters used in the curve fit equation (see Section 4.2) and the R^2 values obtained from curve fitting for the two bridge deck mixes. The values for bridge deck mix A6130 were previously reported by

Myers and Yang (2004) and the values for bridge deck mix A6671 were obtained by curve fitting the raw data obtained from experiments conducted in this study. The value of R^2 for bridge deck mix A6671 is comparable to that of the bridge deck mix A 6130.

Table 5.2 Comparison of Shrinkage-Time Regression Curve Parameters (General Form)

Bridge mix	e	f	e_{shu}	R^2
A 6671	1.0	21	410	0.977
A 6130	1.0	20.8	454	0.987

Figure 5.2 compares the shrinkage results for the HPC deck mix Bridge A6671 to that of Bridge deck mix A6130. The relationship which is shown for both bridge deck mixes represents a comparison of the curve fit equations obtained based on experimental data. It can be observed from Figure 5.2 that the shrinkage strain values for bridge deck mix A6671 was 367.16 and for the bridge deck mix A6130 was 406.97. Shrinkage strain of bridge deck mix A6671 was 9.8% lower than the bridge deck mix A6130. As discussed earlier (see Section 1.1), factors affecting shrinkage include mix composition, curing conditions, member size and shape, water cement ratio etc. As observed from the mix constituents and proportions (see Section 3.2), the coarse aggregate content was 9.9% higher for deck mix A6671 compared to that of deck mix A6130. The course aggregate tends to restrain the paste matrix such that a lower shrinkage strain for deck mix A6671 was somewhat expected and consistent with the test results. Moreover, the w/cm ratio was also an influencing factor for shrinkage, with lower ratios resulting in concrete with lower shrinkage. The w/cm ratio was also lower for deck mix A6671 compared to that of deck mix A6130, resulting in a lower value of shrinkage strain.
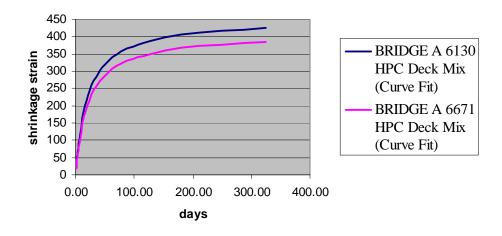
Figure 5.2 Shrinkage Comparison Curve

5.3 Comparison of CTE Results

Table 5.3 and Figure 5.3 illustrate a comparison of CTE results for HPC deck mix A6671 to that of deck mix A6130. In both cases the values are based on laboratory testing of concrete sampled during placement of concrete. The result shows that the value of CTE for bridge A6671 was 3.46% lower than deck mix A6130. The value of CTE for deck mix A6130 was previously reported by Myers and Yang [2004]. The CTE value for deck mix A6671 was obtained from laboratory tests. The variation in CTE seems to be due to the higher amount of coarse aggregate and slag in the deck mix of A6671. The CTE is a function of both the aggregate and the paste. Aggregates generally makes up bulk of the concrete mix and have a higher modulus therefore generally influencing the CTE more significantly. The CTE value is also affected by moisture content. The moisture (water) content is higher in bridge deck mix A6130 also possibly contributing to the slightly higher value of CTE. As the test results for Bridge A6130 is slightly higher, stresses due to thermal expansion and contraction could be expected to be slightly higher.

Table 5.3 average value of CTE for both bridge mixes

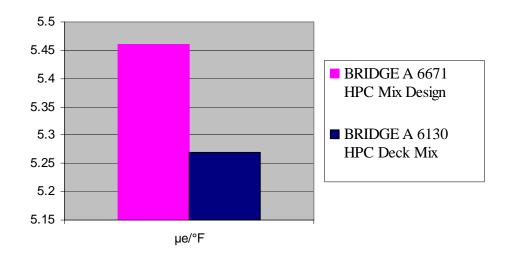|	CTE for A 6130		CTE for A 6671	
Average value of CTE	1/°F	1/°C	1/°F	1/°C
	5.46×10^{-6}	9.83×10^{-6}	5.27×10^{-6}	9.48×10^{-6}

Figure 5.3 CTE Comparison Curve

6. CONCLUSIONS AND RECOMMENDATIONS

This chapter outlines the conclusions based on the testing of specimens for bridge deck mix A6671 and the comparative study of this with bridge deck mix A6130.

The following conclusions were based on the observations from creep, shrinkage and CTE test results of specimens from deck mix A6671:

1. The creep coefficient for deck mix A6671 at 180 days (after curve fitting) was 1.78.

2. The shrinkage strain ($\mu\varepsilon$) at 180 days (after curve fitting) was 367.2.

3. The coefficient of thermal expansion, α_t was observed to be 5.27 x 10^{-6} 1/F (9.48x10^{-6} 1/C).

The following conclusions were based on the comparison study between deck mixes A6130 and A6671:

1. The creep coefficient for deck mix A6671 was 19.3% lower than that of the bridge deck mix A6130. The reason for this higher difference in the creep coefficient may be associated with the higher (9.9%) amount of coarse aggregate, lower amount of cement content and lower w/cm ratio in deck mix of A6671. As noted previously, creep is affected by the aggregate in the concrete, paste matrix, and the w/cm ratio among other factors. Therefore, a higher coarse aggregate content and lower w/cm ratio can be expected to result in a lower creep coefficient, as was the case.

2. Shrinkage strain for deck mix A6671 was 9.8% lower than that of the bridge deck mix A6130. The reason for this was the lower w/cm ratio, lower cement content and higher coarse aggregate content in deck mix A6671. Based on studies we can say that in general lower w/cm ratio with reduced cement content and more coarse aggregate will result in less creep and less shrinkage.

3. CTE for bridge deck mix A6671 is 3.5% lower than that of the bridge deck mix A6130. This apparent variation may be attributed to the difference in the quantity of the coarse aggregates and moisture content used in both mixes.

4. The new deck mix developed by MoDOT and used in Bridge A6671 appears to have preferable SH, CR, and CTE characteristics for a bridge deck application

when compared to the mix design used for Bridge A6130. A reduction in cement for bridge deck applications can aid in reducing or eliminating shrinkage related cracking problems and high stresses developed due to thermal expansion and contraction.

The following recommendations were based on the comparison study between deck mixes A6130 and A6671:

1. A reduction in the cement content for bridge deck applications is recommended based on the mix designs investigated in this study to aid in reducing or eliminating shrinkage related cracking problems.

2. A higher percentage of coarse aggregate is recommended assuming placement and workability requirements can be met to aid in reducing the overall shrinkage of a concrete mix based on the mix designs investigated in this study.

REFERENCES

American Association of State Highway and Transportation Officials, AASHTO LRFD Bridge Design Specifications, First Edition, 1994.

American Association of State Highway and Transportation Officials, Standard Specifications for Highway Bridges, Sixteenth Edition, 1996.

ACI Committee 209, "Prediction of Creep, Shrinkage, and Temperature Effects in Concrete Structures," ACI 209R-92, American Concrete Institute, Detroit, 1992.

ACI Committee 363, "State-of-the-Art Report on High-Strength Concrete," ACI 363R-92, American Concrete Institute, Detroit, 1992.

American Society for Testing and Materials, "Standard Test Method for Creep of Concrete in Compression," ASTM C512-87(1992)e1, ASTM, West Conshohocken, Pennsylvania, 1992.

ASTM Standards C 109, "Standard Test Methods for Compressive Strength of Hydraulic Cement Mortars", 2002.

Bazant, Z. P. and Panula, L., "Creep and Shrinkage Characterization for Analyzing Prestressed Concrete Structures," PCI Journal, May/June 1980, Vol. 15, No. 3, pp. 87-122.

Branson, D. E. and Christiason, M. L., "Time-Dependent Concrete Properties Related to Design – Strength and Elastic Properties, Creep, and Shrinkage," ACI Special Publication SP-27, Creep, Shrinkage, and Temperature Effects in Concrete Structures, American Concrete Institute, Detroit, 1971.

Branson, D. E. and Kripanarayanan, K. M., "Loss of Prestress, Camber, and Deflection of Non-composite and Composite Prestressed Concrete Structures," PCI Journal, September/October 1971, Vol. 16, No. 5, pp. 22-52.

Brooks, J. J. and Neville, A., "Creep and Shrinkage of Concrete as Affected by Admixtures and Cement Replacement Materials," Creep and Shrinkage of Concrete: Effect of Materials and Environment, ACI SP 135, American Concrete Institute, Detroit, 1992, pp. 19-36.

Comite Euro-International du Beton (CEB), CEB-FIP International Recommendations for the Design and Construction of Concrete Structures, Paris-London, 1970.

Comite Euro-International du Beton (CEB), CEB-FIP Model Code 1990, Final Draft, Lausanne, 1991.

CTE Quarterly Report, "Creep, Shrinkage and CTE Evaluation", September 2003, RI00-002B.

Myers, J.J., and Yang, Y., "Field and laboratory Performance of Prestressed Concrete Girders for MO Bridge Structures", MODoT, RDT -04-016, June 2004.

El Hindy, E., Miao, B., Chaallal, O., and Aitcin, P.-C., "Drying Shrinkage of Ready-Mixed High Performance Concrete," ACI Materials Journal, May/June 1994, Vol. 91, No. 3, pp. 300-305.

Gilbert, R. I., Time Effects in Concrete Structures, Elsevier Science Publishers, Amsterdam, 1988.

Hansen, T. C. and Mattock, A. H., "Influence of Size and Shape of Member on the Shrinkage and Creep of Concrete," ACI Journal, February 1966, Vol. 63, No. 2, pp. 267-289.

Hanson, J. A., "Prestress Loss as Affected by Type of Curing," PCI Journal, April 1964, Vol. 9, No. 2, pp. 69-93.

Klieger, P., Some Aspects of Durability and Volume Change of Concrete for Prestressing, Research Development Bulletin 118, Portland Cement Association, Skokie, Illinois, 1960.

Libby, J. R., Modern Prestressed Concrete, Fourth Edition, Van Nostrand Reinhold, New York, 1990.

McDonald, D., "Development of a Simplified Code Procedure for the Prediction of Shrinkage and Creep," Creep and Shrinkage of Concrete – Proceedings of the Fifth International RILEM Symposium, International Union of Testing and Research Laboratories for Materials and Structures (RILEM), Cambridge, 1993.

Mindess, S. and Young, J. F., Concrete, Prentice-Hall, Englewood Cliffs, New Jersey, 1981.

MoDOT, "Laboratory Study – Laboratory Testing of Bridge deck Mixes", RI01-044, March 2003

Muller, H. S., "New Prediction Models for Creep and Shrinkage of Concrete," Creep and Shrinkage of Concrete: Effect of Materials and Environment, ACI SP 135, American Concrete Institute, Detroit, 1992, pp. 1-18.

Nasser, K. W. and Al-Manaseer, A. A., "Creep of Concrete Containing Fly Ash and Superplasticizer at Different Stress/Strength Ratios," ACI Journal, July/August 1986, Vol. 83, No. 4, pp. 668-673.

Neville, A. M., Dilger, W. H., and Brooks, J. J., Creep of Plain and Structural Concrete, Longman Group, 1983.

Neville, A. M., Properties of Concrete, Third Edition, Pitman Publishing, London, 1981

Ngab, A. S., Nilson, A. H., and Slate, F. O., "Shrinkage and Creep of High Strength Concrete," ACI Journal, July/August 1981, Vol. 78, No. 4, pp. 255-261.

Nilson, A. H. and Winter, G., Design of Concrete Structures, Eleventh Edition, McGraw-Hill, New York, 1991.

Parrot, L. J., "The Properties of High-Strength Concrete," Technical Report No. 42.417, Cement and Concrete Association, Wexham Springs, 1969.

Sennour, M. L. and Carrasquillo, R. L., Creep and Shrinkage Properties in Concrete Containing Fly Ash, Research Report 481-6, Center for Transportation Research, The University of Texas at Austin, Austin, Texas, 1989.

Smadi, M. M., Slate, F. O., and Nilson, A. H., "Shrinkage and Creep of High-, Medium-, and Low-Strength Concretes, Including Overloads, ACI Materials Journal, May/June 1987, Vol. 84, No. 3, pp. 224-234.

Swamy, R. N. and Anand, K. L., "Shrinkage and Creep Properties of High Strength Structural Concrete," Civil Engineering and Public Works Review (London), October 1973, Vol. 68, No. 807, pp. 859-868.

Chojnacki, T., MoDOT Mix Design report, Tuesday June 22, 2004 via email correspondence.

Troxell, G. E., Davis, H. E., and Kelly, J. W., Composition and Properties of Concrete, Second Edition, McGraw-Hill, New York, 1968.